Journal of Pharmacological Sciences 145 (2021) 97–104

Contents lists available at ScienceDirect

Journal of Pharmacological Sciences

journal homepage: www.elsevier.com/locate/jphs

Full Paper

Ramelteon modulates gamma oscillations in the rat primary motor cortex during non-REM sleep

Airi Yoshimoto [a, b], Kotaro Yamashiro [a], Takeshi Suzuki [b], Yuji Ikegaya [a, c, d], Nobuyoshi Matsumoto [a, *]

[a] Graduate School of Pharmaceutical Sciences, The University of Tokyo, Tokyo 113-0033, Japan
[b] Graduate School of Pharmaceutical Sciences, Keio University, Tokyo 105-8512, Japan
[c] Center for Information and Neural Networks, National Institute of Information and Communications Technology, Suita City, Osaka 565-0871, Japan
[d] Institute for AI and Beyond, The University of Tokyo, Tokyo 113-0033, Japan

ARTICLE INFO

Article history:
Received 14 October 2020
Accepted 12 November 2020
Available online 20 November 2020

Keywords:
Ramelteon
Rat
Electrocorticogram
Sleep
Gamma oscillation

ABSTRACT

Sleep disorders adversely affect daily activities and cause physiological and psychiatric problems. The shortcomings of benzodiazepine hypnotics have led to the development of ramelteon, a melatonin MT_1 and MT_2 agonist. Although the sleep-promoting effects of ramelteon have been documented, few studies have precisely investigated the structure of sleep and neural oscillatory activities. In this study, we recorded electrocorticograms in the primary motor cortex, the primary somatosensory cortex and the olfactory bulb as well as electromyograms in unrestrained rats treated with either ramelteon or vehicle. A neural-oscillation-based algorithm was used to classify the behavior of the rats into three vigilance states (*e.g.*, awake, rapid eye movement (REM) sleep, and non-REM (NREM) sleep). Moreover, we investigated the region-, frequency- and state-specific modulation of extracellular oscillations in the ramelteon-treated rats. We demonstrated that in contrast to benzodiazepine treatment, ramelteon treatment promoted NREM sleep and enhanced fast gamma power in the primary motor cortex during NREM sleep, while REM sleep was unaffected. Gamma oscillations locally coordinate neuronal firing, and thus, ramelteon modulates neural oscillations in sleep states in a unique manner and may contribute to off-line information processing during sleep.

1. Introduction

Adequate sleep is fundamental for all mammals, and sleep deficits cause physiological and psychiatric disorders. Sedative hypnotics mainly consisting of benzodiazepines (*e.g.*, triazolam and brotizolam) and nonbenzodiazepines (*e.g.*, zolpidem, zopiclone, and zaleplon, called Z-drugs) have been widely used to ameliorate sleep debt or insomnia. Although these hypnosedative drugs have reliable sleep-promoting effects, they are accompanied by severe side effects such as sleep hangover, anterograde amnesia, rebound insomnia, cognitive impairment, drug dependency and tolerance.[1–5] To overcome this problem, drugs that promote sleep in a manner different from benzodiazepines have been developed. For example, one type of drug acts through melatonin MT_1 and MT_2 receptors expressed in the suprachiasmatic nucleus.[6–8]

Ramelteon, one of these melatonin receptor agonists, has a high affinity for MT_1 and MT_2 receptors and moderately promotes sleep.[9–13] Although ramelteon has been proven safe and effective for managing chronic insomnia,[14] the physiological effects of ramelteon on neural oscillations have been poorly investigated thus far. Previous studies have described the impact of ramelteon on neural oscillations of rats and monkeys, but the studies focused on low-frequency (<30 Hz) oscillations.[10,15] While low-frequency oscillations are capable of traveling further distances, high-frequency (>60 Hz) neocortical oscillations during sleep locally coordinate neuronal firing and are believed to be important for neural plasticity and behavioral functions such as cognition and perception, as shown in rodents, monkeys and humans.[16–20] However, it remains

* Corresponding author. Laboratory of Chemical Pharmacology, Graduate School of Pharmaceutical Sciences, The University of Tokyo, 7-3-1 Hongo, Bunkyo-ku, Tokyo 113-0033, Japan. Fax: +81 3 5841 4786.
E-mail address: nobuyoshi@matsumoto.ac (N. Matsumoto).
Peer review under responsibility of Japanese Pharmacological Society.

https://doi.org/10.1016/j.jphs.2020.11.006

unclear whether high-frequency neural oscillations in the neocortex are modulated by ramelteon treatment.

To address this issue, we simultaneously recorded electrocorticograms (ECoGs) from the primary motor cortex (M1), the primary somatosensory cortex (S1) and the olfactory bulb (OB) in unrestrained and ramelteon- and vehicle-treated rats with nuchal electromyograms (EMGs).[21–23] Using neural oscillatory activity in the OB and M1, we classified rat behavior into three vigilance states (awake, rapid eye movement (REM) sleep, and non-REM (NREM) sleep). We then investigated the modulation of extracellular oscillations in the ramelteon-treated animals during REM and NREM sleep.

2. Materials and methods

2.1. Ethical approval

The animal experiments were performed with the approval of the Animal Experiment Ethics Committee at The University of Tokyo (approval number: P29-7) and according to the University of Tokyo guidelines for the care and use of laboratory animals. These experimental protocols were carried out in accordance with the Fundamental Guidelines for the Proper Conduct of Animal Experiments and Related Activities in Academic Research Institutions (Ministry of Education, Culture, Sports, Science and Technology, Notice No. 71 of 2006), the Standards for Breeding and Housing of and Pain Alleviation for Experimental Animals (Ministry of the Environment, Notice No. 88 of 2006) and the Guidelines on the Method of Animal Disposal (Prime Minister's Office, Notice No. 40 of 1995). All efforts were made to minimize animal suffering.

2.2. Animals

A total of eight male 8- to 10-week-old Wistar rats (Japan SLC, Shizuoka, Japan) with a preoperative weight of 180–300 g were housed individually under conditions of controlled temperature and humidity (22 ± 1 °C, 55 ± 5%) and maintained on a 12:12-h light/dark cycle (lights off from 7:00 to 19:00) with *ad libitum* access to food and water. The rats were habituated to an experimenter via daily handling for 2 d before the experiments.

2.3. Preparation

A recording interface assembly was prepared as previously described.[21–23] In short, the assembly was composed of an electrical interface board (EIB) (EIB-36-PTB, Neuralynx, Inc., Bozeman, MT, USA) and custom-made shell and core bodies by three-dimensional (3-D) printers (UP Plus2, Tiertime, Beijing, China; Formlabs Form 2, Formlabs, Somerville, MA, USA). The EIB had a sequence of metal holes for connections with wire electrodes. A given individual hole was conductively connected with one end of the insulated wire (~5 cm) using attachment pins, whereas the opposite end was soldered to a corresponding individual electrode during surgery.

2.4. Surgery

General anesthesia was induced in the rats and maintained with 2–3% and 1–2% isoflurane gas, with careful inspection of the animal's condition during the whole surgical procedure. Veterinary ointment was applied to the rat's eyes to prevent drying. The skin was sterilized with povidone iodine and 70% ethanol whenever we made an incision.

After anesthesia, the electrodes for EMGs were implanted as described previously.[21–24] Briefly, we mounted the rat onto a stereotaxic apparatus (SR-6R-HT, Narishige, Tokyo, Japan) according to the general surgical procedure.[25] One wire electrode (AS633, Cooner Wire, CA, USA) was implanted into the trapezius to record EMGs. The scalp was then removed with a surgical knife. A circular craniotomy with a diameter of approximately 0.9 mm was performed using a high-speed dental drill (SD-102, Narishige). Epidural stainless-steel screws (1.4 mm in diameter, 3 mm in length) were used to record ECoGs from the S1 and M1, whereas a smaller screw electrode (1.0 mm in diameter, 4 mm in length) was used to record ECoGs from the OB. The six screw electrodes were stereotaxically implanted bilaterally into the S1 (2.1 mm posterior and 2.8 mm lateral to the bregma), M1 (3.2 mm anterior and 3.0 mm lateral to the bregma) and the OB (10.0 mm anterior and 1.0 mm lateral to the bregma); notably, the coordinates for M1 in this study were previously referred to as those for the frontal cortex,[26–29] and the coordinates were used to probe vigilance states.[28,29] In addition, another two stainless-steel screws were implanted into the bone above the cerebellum (9.6 mm anterior and 1.0 mm bilateral to the bregma) as ground and reference electrodes. Each of the open edges of the electrodes was soldered to the corresponding open edge of the insulated wires of the recording interface assembly. This assembly, which included the electrodes, was secured to the skull using dental cement.

Following surgery, each rat was allowed to recover from anesthesia and was housed individually in transparent plexiglass cages with free access to water and food. For the first 2 d after surgery, we carefully assessed the condition of the animals every 3 h except during the night (*i.e.*, 20:00 to 8:00). Then, their conditions were assessed with an interval of <6 h at least 3 times a day. The animals were habituated to the experimenter again by handling for 5 d after surgery. In addition, we manually monitored the physical condition, behavior, and water and food intake every day after surgery. After we confirmed that all these monitored data satisfied our criteria, we commenced the electrophysiological recordings. We set 5 or more (typically, 10-14) days as the post-recovery period.

While our experimental protocols mandate the humane killing of animals if they exhibit any signs of pain, prominent lethargy or discomfort, we did not observe such symptoms in any of the 8 rats used in this study.

2.5. Apparatus

The open field used in this study measured 40 cm in width, 40 cm in depth, and 40 cm in height.[30] The walls were made of black-painted wood. For habituation, each rat was placed in the open field arena and was allowed to freely explore it for 6 h for approximately 7 d.

2.6. Drug

Ramelteon (184-03371, Fujifilm Wako, Osaka, Japan) was dissolved in DMSO at a concentration of 200 mg/ml. This solution was diluted 100 times with saline solution to a final concentration of 2 mg/ml immediately before use. Saline with 1% DMSO was used as the vehicle control solution.

2.7. In vivo electrophysiology

After the rats fully recovered from surgery and became familiar with the open arena, we performed electrophysiological recordings for two days. We started the experiments at 9:30 a.m. for either day. On the first day, each rat was gently placed in the open field, and the recording electrode assembly was connected to a digital low-noise amplifier (C3324, Intan Technologies, CA, USA). The output of the headstage was conducted through SPI cables (C3216, Intan Technologies) and a commutator to the acquisition board (Open Ephys, MA,

USA[31]). We recorded ECoGs and EMGs for 3 h. Following the recordings, either vehicle or ramelteon (5 ml/kg for both) was intraperitoneally administered to each rat. Immediately (~10 min) after administration, we placed each rat in the open arena and recorded the ECoGs and EMGs for 3 h. On the second day, we performed the same experiment with the other drug, either vehicle or ramelteon, in a randomized crossover design. For all the recordings, the electrophysiological signals were amplified and digitized at 2 kHz.

2.8. Histology

After the recordings, the rats were anesthetized with an overdose of isoflurane gas and transcardially perfused with 4% paraformaldehyde (PFA) in 0.01 M phosphate-buffered saline (pH 7.4), followed by decapitation. The brains were soaked overnight in 4% PFA for post-fixation and coronally sectioned at a thickness of 100 μm using a vibratome (DTK-1000N, Dosaka EM, Kyoto, Japan). Acute serial slices were mounted on glass slides and processed for cresyl violet staining. For cresyl violet staining, the slices were rinsed in water, ethanol and xylene, counterstained with cresyl violet, and coverslipped with a mounting agent (PARAmount-D, Falma, Tokyo, Japan). The positions of all screw electrodes were confirmed by identifying dents on the superficial layer in the histological tissue. Data were excluded from the subsequent analysis if the electrode position was outside the target brain region. Cresyl violet-stained images were acquired using a phase-contrast microscope (BZ-X710, Keyence, Osaka, Japan).

2.9. Data analysis

All data analyses were performed using custom-made MATLAB routines (MathWorks, MA, USA). The summarized data are reported as the mean ± the standard error of the mean (SEM). The null hypothesis was statistically rejected when $P < 0.05$, unless otherwise specified.

The recording periods dominated by apparent electrical noise caused by a physical impact when a rat hit its head on the walls were manually excluded from the analysis. To define awake and sleep states, we first divided the recording periods into 5-s segments. We bandpass filtered the OB ECoGs into gamma (50–70 Hz) frequency bands using fast Fourier transform (FFT) and further convoluted the ECoG signals with a complex Morlet wavelet family (bandwidth parameter, 1.5; center frequency, 2).[32] We calculated the gamma power for each segment to obtain the consecutive gamma power signal.[33] We then detected the two vigilance states by applying the gamma signal to a Schmitt trigger circuit with two thresholds, followed by *post hoc* adjustments with the aid of the experimenter's notebook if necessary.[34] We calculated the ratio of the absolute time spent sleeping to each time bin (*e.g.*, 30 min for Fig. 2E) and defined the value as the (relative) sleep time. We further employed the difference in the value before and after drug injection, which is hereafter signified by Δ. Brief (<120 s) sleep bouts were defined as fragmented sleep episodes.[35]

We next calculated the ratio of the power in the delta band (0.3–4 Hz) to the theta band (4–8 Hz) from M1 ECoGs for each 5-s segment to obtain the consecutive delta-theta ratio signal. We further classified sleep states into the REM and NREM sleep states based on the delta-theta ratio, followed by cross-validation with visual inspection of the power spectra and raw ECoG traces, if needed.[34] We then evaluated the (relative) NREM and REM sleep times.

To better understand the neural oscillatory activity, we transformed the M1 and S1 ECoG signals during the NREM and REM sleep bouts into frequency spectra using FFT. We then calculated

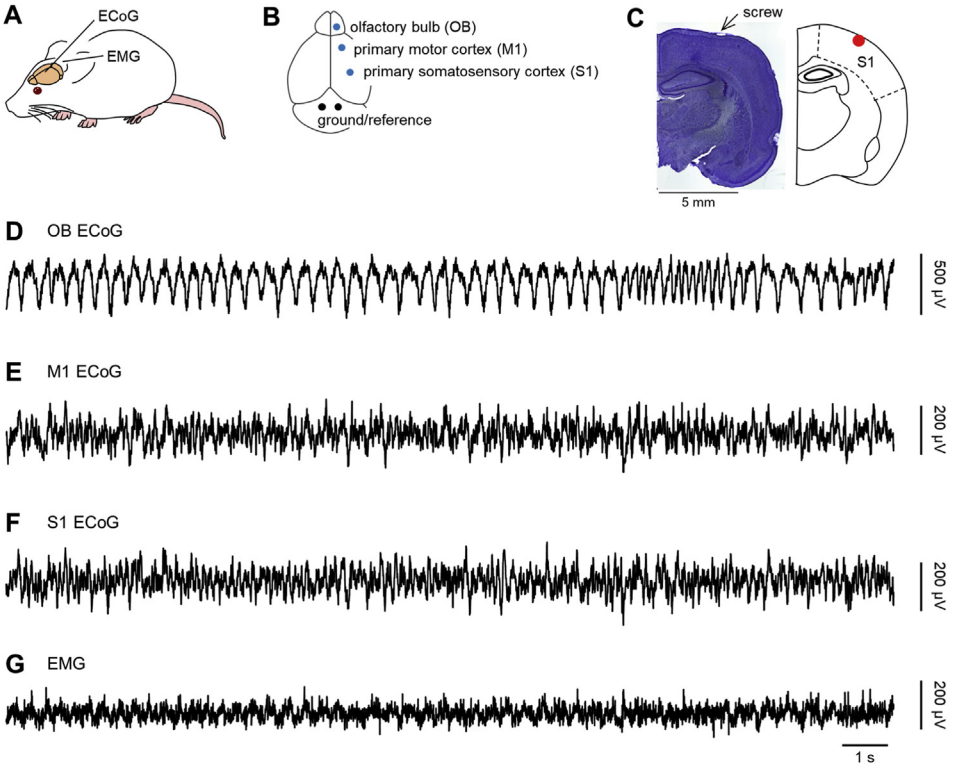

Fig. 1. Simultaneous recordings of multisite ECoGs and EMGs. ***A***, A diagram of the experimental setup. ***B***, A top–view diagram of the ECoG recording sites (OB, M1, and S1, *blue*) and ground/reference sites (*black*). ***C***, Representative *post hoc* histology of the recording site. ***D***, A representative trace of ECoGs in the OB. ***E***, The same as *D*, but for ECoGs in the M1. ***F***, The same as *D*, but for ECoGs in the S1. ***G***, The same as *D*, but for EMGs. *Abbreviations*: ECoG, electrocorticogram; EMG, electromyogram; OB, olfactory bulb; M1, primary motor cortex; S1, primary somatosensory cortex.

the power in specific frequency bands (*e.g.*, delta (0.3–4 Hz), theta (4–8 Hz), beta (15–30 Hz), slow gamma (30–60 Hz), and fast gamma (60–90 Hz)) as the area under the spectra between corresponding frequencies.[36,37]

3. Results

We simultaneously recorded ECoGs in the S1, M1 and OB and EMGs in freely behaving rats before and after treatment with either vehicle or ramelteon in a randomized crossover manner (Fig. 1). We then bandpassed the OB ECoGs in the gamma frequency range (Fig. 2A, B). Based on the power of the gamma oscillations in the OB ECoGs,[33] we divided the recording periods into the sleep and awake states (Fig. 2C, D). Time-course analysis of the sleep time revealed that the rats gradually spent more time sleeping after intraperitoneal administration of ramelteon but not vehicle ($P = 0.1$, $JT = 1.30$ (vehicle), $P = 0.01$, $JT = 2.28$ (ramelteon), Jonckheere-Terpstra trend test; Fig. 2E). Overall, ramelteon significantly increased the amount of sleep compared with the vehicle (−10.1 ± 4.0% (vehicle) *vs.* 6.8 ± 2.4% (ramelteon), $P = 0.01$, $t_7 = 3.31$, $n = 8$ rats, paired *t*-test; Fig. 2F). Because sleep fragmentation is related to a risk of neuroinflammation,[38] we quantified the incidence of fragmented sleep before and after the vehicle and ramelteon treatments, but there was no significant difference in the increment of the incidents between the two conditions (3.2 ± 1.8 events/h (vehicle) *vs.* −0.7 ± 0.7 events/h (ramelteon), $P = 0.14$, $t_7 = 1.65$, $n = 8$ rats, paired *t*-test; Fig. 2G).

We bandpassed the M1 ECoGs in the delta and theta frequency ranges (Fig. 3A, B). Based on the delta-to-theta power ratio (see Materials and methods), we further divided the sleep states into the REM and NREM periods (Fig. 3C, D). Time-course analysis revealed that vehicle administration was likely to slightly decrease the NREM sleep time, whereas ramelteon increased the time spent in NREM sleep (Fig. 3E), yielding a significant increment of NREM sleep in the ramelteon-treated condition compared with the vehicle-treated condition (−7.3 ± 5.2% (vehicle) *vs.* 4.7 ± 3.4% (ramelteon), $P = 0.04$, $t_5 = 2.72$, $n = 6$ rats, paired *t*-test; Fig. 3F). As in the case of NREM sleep, time-course analysis also confirmed that REM sleep bouts were gradually reduced and increased after the administration of vehicle and ramelteon, respectively (Fig. 3G); however, there was no significant difference in either the increment or decrement of REM sleep bouts between the two conditions (3.7 ± 6.2% (vehicle) *vs.* 1.1 ± 3.4% (ramelteon), $P = 0.77$, $t_5 = 0.31$, $n = 6$ rats, paired *t*-test; Fig. 3H).

To further investigate how ramelteon modulates cortical neural activity during REM and NREM sleep, we estimated the power density of the spectral components of the S1 and M1 in the vehicle- and ramelteon-treated conditions using FFT (Fig. 4A–D). The powers of slow and fast gamma oscillations in the M1 were likely to increase during both REM and NREM sleep (Fig. 4E, F, Table 1). Specifically, fast gamma oscillations in the M1 were significantly enhanced when ramelteon was administered compared with vehicle (Fig. 4E). In contrast, there was no significant difference in fast or slow gamma power in the S1 during REM and NREM sleep

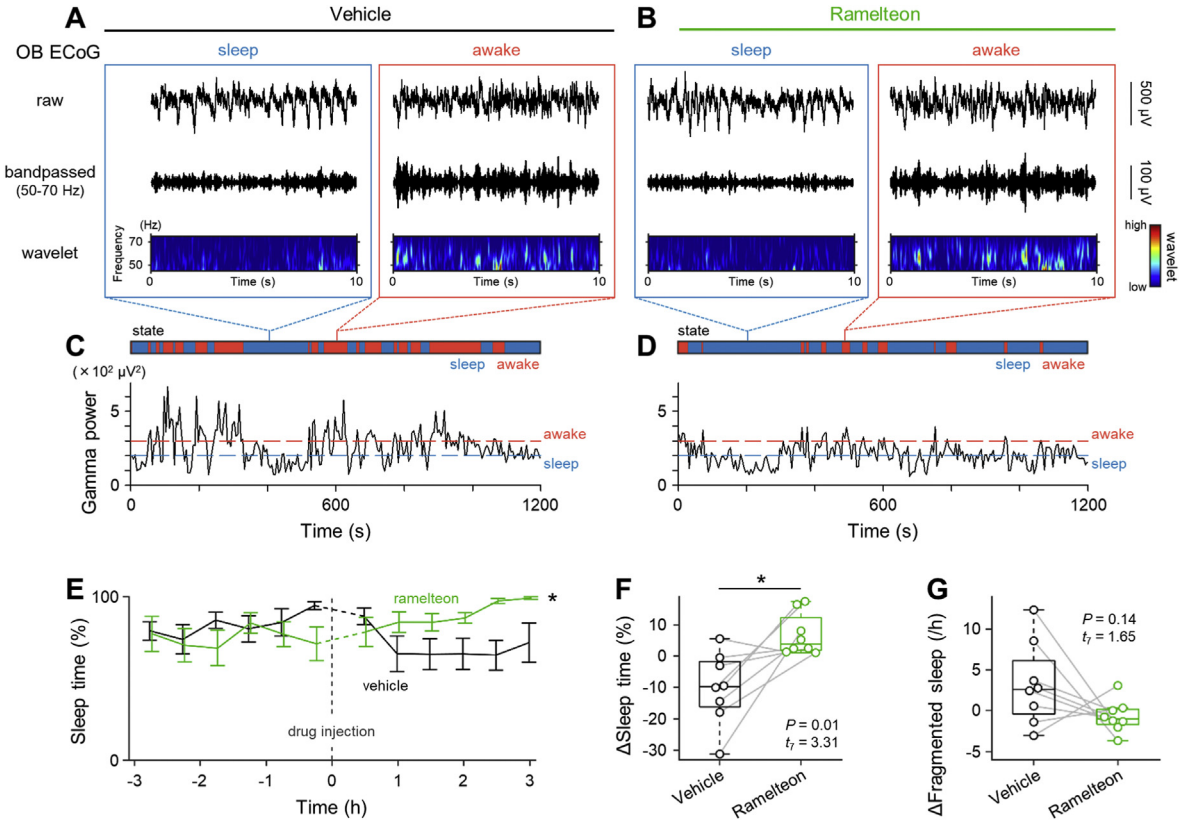

Fig. 2. Promotion of sleep time after ramelteon administration. ***A***, *Left*: Representative raw (*top*) and bandpass filtered (50–70 Hz, *middle*) traces of ECoGs in the OB during the sleep state in the vehicle-treated rats. The *top* trace was convoluted with a Morlet wavelet family and transformed into the pseudo-colored matrix in a time-frequency domain (*bottom*). *Right*: The same as *left*, but for the awake state. ***B***, The same as *A*, but for the ramelteon-treated rats. ***C***, Awake and sleep states (*red* and *blue*, respectively (*top*)) were defined based on the time-course transitions of the gamma (50–70 Hz) power of OB ECoGs in the vehicle-treated condition (*bottom*). ***D***, The same as *C*, but for the ramelteon-treated condition. ***E***, Relative sleep time was scored every 30 min before and after drug (*e.g.*, vehicle (black) and ramelteon (*green*)) administration. Statistics were compiled by the Jonckheere-Terpstra trend test. ***F***, The increment of sleep time (ΔSleep time) was quantified in both conditions. ***G***, The increment of the event rate of sleep fragmentation. The *P* and *t* values were obtained by paired *t*-tests, with $n = 8$ rats for *F* and *G*. *Abbreviations*: ECoG, electrocorticogram; OB, olfactory bulb.

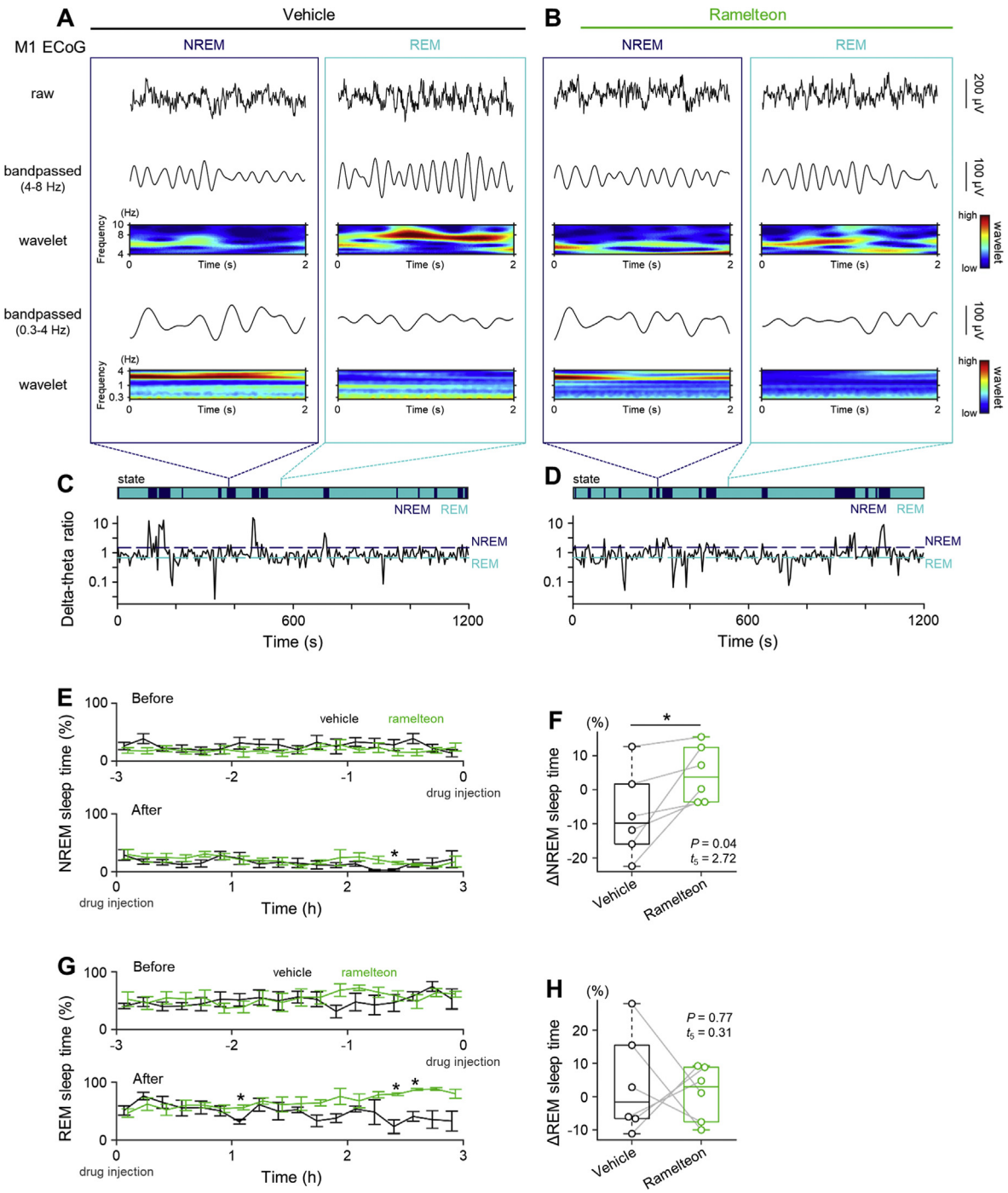

Fig. 3. Promotion of the NREM but not REM sleep time after ramelteon administration. ***A***, *Left*: Representative raw (*first row*) and bandpass filtered (4–8 Hz and 0.3–4 Hz (*second* and *fourth*, respectively)) traces of ECoGs in the M1 during the NREM sleep state in the vehicle-treated rats. The *first* trace was convoluted with a Morlet wavelet family and transformed into pseudo-colored matrices in the time-frequency domain (*third* and *fifth*). *Right*: The same as *left*, but for the REM sleep state. ***B***, The same as *A*, but for the ramelteon-treated rats. ***C***, NREM and REM states (*navy blue* and *pale blue*, respectively (*top*)) were detected based on the time-course transitions of the ratio of delta (0.3–4 Hz) power to theta (4–8 Hz) power in the M1 ECoGs in the vehicle-treated condition (*bottom*). ***D***, The same as *C*, but for the ramelteon-treated condition. ***E***, *Top*: Relative NREM sleep time was scored every 10 min before drug (*e.g.*, vehicle (*black*) and ramelteon (*green*)) administration. *Bottom*: The same as *top*, but for after drug administration. ***F***, The increment of NREM sleep time (ΔNREM sleep time) was quantified in both conditions. ***G***, The same as *E*, but for the REM sleep time. ***H***, The same as *F*, but for the REM sleep time. Statistics were assessed by Student's *t*-test for *E* and *G*. The *P* and *t* values were obtained by paired *t*-tests, with $n = 6$ rats for *F* and *H*. *Abbreviations*: ECoG, electrocorticogram; M1, primary motor cortex; REM, rapid eye movement; NREM, non-rapid eye movement.

between the two conditions (Fig. 4G, H, Table 1). We did not find any significant differences in the oscillation power in other frequency bands (*e.g.*, delta, theta, and beta) in either the cortex during REM or NREM sleep between the two conditions (Fig. S1, Table 1).

4. Discussion

In this study, we found that ramelteon treatment promoted average sleep time, especially NREM sleep bouts, for 3 h after ramelteon administration. Moreover, our spectral analyses on

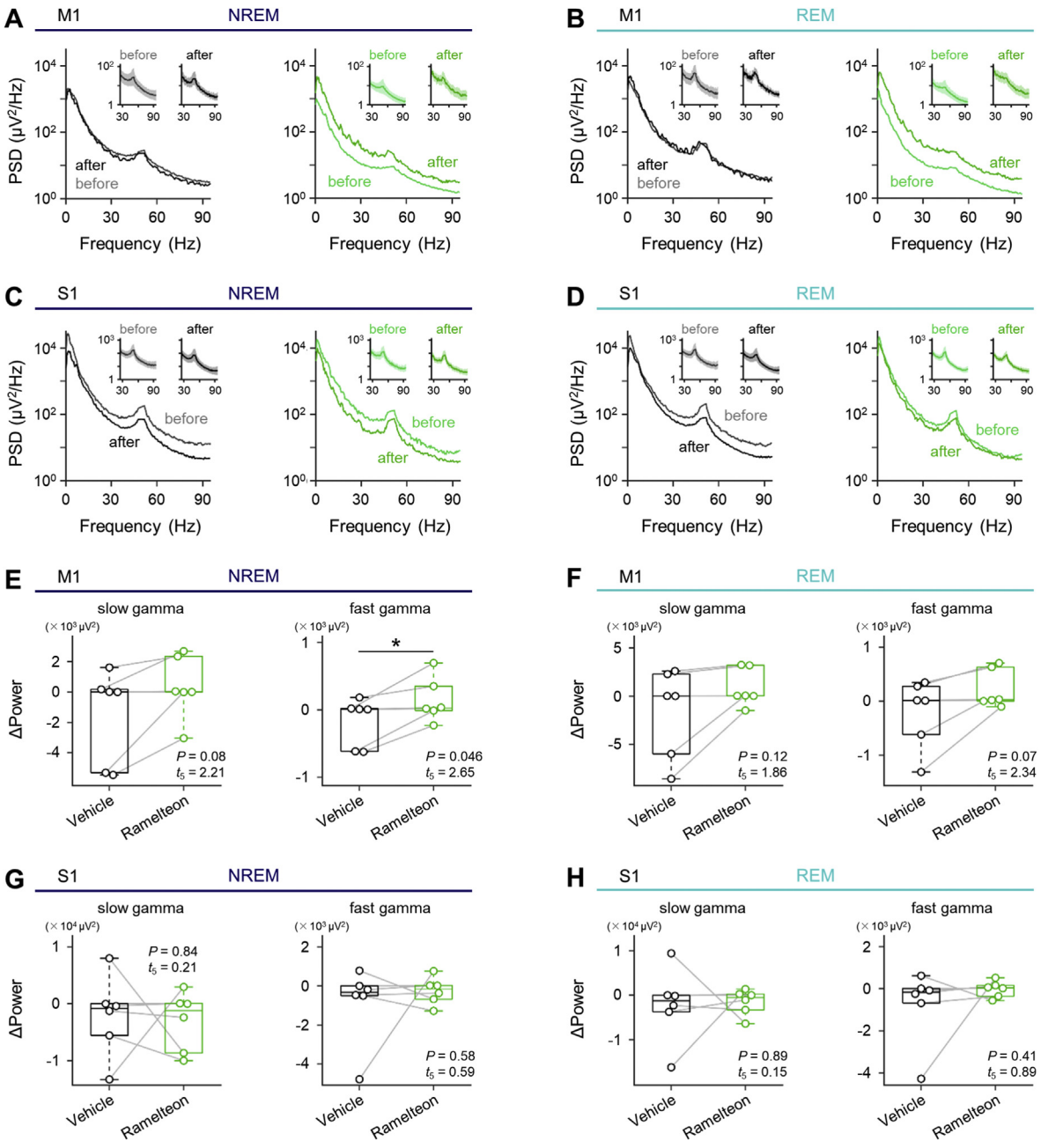

Fig. 4. Region-, frequency- and state-specific modulation of extracellular oscillations in the ramelteon-treated rats. ***A***, *Left*: Power spectral densities of ECoGs in the M1 during NREM sleep before (*gray*) and after (*black*) vehicle administration. The spectrum at 30–90 Hz (*i.e.*, gamma frequency band) is displayed in the *inset*. *Right*: The same as *left*, but for before (*jade*) and after (*green*) ramelteon administration. ***B***, The same as *A*, but for REM sleep. ***C***, The same as *A*, but for the S1. ***D***, The same as *C*, but for REM sleep. ***E***, *Left*: The increment of slow gamma power in the M1 during NREM sleep in the vehicle- and ramelteon-treated conditions (*black* and *green*, respectively). *Right*: The same as *left*, but for fast gamma power. ***F***, The same as *E*, but for REM sleep. ***G***, The same as *E*, but for the S1. ***H***, The same as *G*, but for REM sleep. The *P* and *t* values were obtained by paired *t*-tests, with $n = 6$ rats for *E-H*. *Abbreviations*: PSD, power spectral density; M1, primary motor cortex; S1, primary somatosensory cortex; REM, rapid eye movement; NREM, non-rapid eye movement.

cortical neural activity demonstrated that fast gamma oscillations in the M1 were enhanced during NREM sleep when ramelteon was administered compared with vehicle. These results suggest that ramelteon simply promotes average NREM sleep episodes, which might be mediated by MT_2 receptors.[39]

The view that wakefulness is a state in which whole cortical neurons are persistently activated and desynchronized is widely accepted. Consequently, it is believed that EEGs are dominated by low-amplitude, high-frequency oscillations when animals are awake. However, a previous study classified sleep and awake states based on cortical delta waves and EMGs, demonstrating that neuronal activities during brief periods (5–15 min) from awakening were silent, called OFF periods included in quiet awake states. These OFF periods could not be detected based on either cortical delta waves or EMGs.[40] Moreover, another recent study suggested that EMG activities conflated sleep and quiet awake states in some cases and demonstrated that olfactory gamma power resolved this issue.[33] If we had utilized the powers of cortical slow waves and EMGs, we could indeed have discriminated quiet awake episodes from NREM sleep episodes to a large extent. However, we could not have excluded the possibility that the OFF periods were overlooked, and quiet awake states were thereby underestimated. We thus

Table 1
All statistical values regarding ΔPower. (related to Fig. 4 and Supplementary Figure 1).

M1 (NREM)	Vehicle	Ramelteon	Statistics	
	ΔPower (μV^2)	ΔPower (μV^2)	*P*	t_5
Delta	0.9 ± 2.0 ($\times 10^5$)	0.8 ± 8.2 ($\times 10^5$)	0.93	0.09
Theta	-3.6 ± 5.4 ($\times 10^4$)	2.6 ± 2.2 ($\times 10^4$)	0.23	1.37
Beta	-2.3 ± 3.0 ($\times 10^3$)	1.8 ± 1.3 ($\times 10^3$)	0.13	1.78
Slow gamma	-1.5 ± 1.3 ($\times 10^3$)	0.4 ± 0.8 ($\times 10^3$)	0.08	2.21
Fast gamma	-1.7 ± 1.4 ($\times 10^2$)	1.4 ± 1.3 ($\times 10^2$)	0.046	2.65
M1 (REM)	Vehicle	Ramelteon	Statistics	
	ΔPower (μV^2)	ΔPower (μV^2)	*P*	t_5
Delta	1.5 ± 2.4 ($\times 10^5$)	1.1 ± 0.9 ($\times 10^5$)	0.82	0.24
Theta	-2.1 ± 5.5 ($\times 10^4$)	3.7 ± 2.7 ($\times 10^4$)	0.25	1.32
Beta	-2.3 ± 4.1 ($\times 10^3$)	2.6 ± 1.6 ($\times 10^3$)	0.22	1.42
Slow gamma	-1.6 ± 1.9 ($\times 10^3$)	0.8 ± 0.8 ($\times 10^3$)	0.12	1.86
Fast gamma	2.2 ± 2.6 ($\times 10^2$)	2.1 ± 1.5 ($\times 10^2$)	0.07	2.34
S1 (NREM)	Vehicle	Ramelteon	Statistics	
	ΔPower (μV^2)	ΔPower (μV^2)	*P*	t_5
Delta	2.4 ± 3.0 ($\times 10^5$)	-0.4 ± 2.6 ($\times 10^5$)	0.61	0.55
Theta	3.2 ± 9.8 ($\times 10^4$)	-2.1 ± 3.3 ($\times 10^4$)	0.69	0.42
Beta	-1.2 ± 5.2 ($\times 10^3$)	-6.9 ± 3.8 ($\times 10^3$)	0.49	0.74
Slow gamma	-2.1 ± 2.9 ($\times 10^3$)	-3.0 ± 2.1 ($\times 10^3$)	0.84	0.21
Fast gamma	-8.6 ± 8.1 ($\times 10^2$)	-2.5 ± 2.9 ($\times 10^2$)	0.58	0.59
S1 (REM)	Vehicle	Ramelteon	Statistics	
	ΔPower (μV^2)	ΔPower (μV^2)	*P*	t_5
Delta	3.4 ± 2.9 ($\times 10^5$)	-0.1 ± 2.2 ($\times 10^5$)	0.47	0.78
Theta	7.7 ± 9.9 ($\times 10^4$)	1.9 ± 4.8 ($\times 10^4$)	0.65	0.48
Beta	-1.7 ± 4.5 ($\times 10^3$)	-1.9 ± 3.6 ($\times 10^3$)	0.98	0.03
Slow gamma	-2.2 ± 3.4 ($\times 10^3$)	-1.5 ± 1.2 ($\times 10^3$)	0.89	0.15
Fast gamma	-7.8 ± 7.2 ($\times 10^2$)	-0.3 ± 1.6 ($\times 10^2$)	0.41	0.89

Statistics are compiled by paired *t*-tests ($n = 6$ rats).

adopted a motor-activity-independent scoring method to distinguish two (*e.g.*, awake and sleep) states using the OB ECoGs (Fig. 2A–D).[33] We then quantified the time spent sleeping in each 30-min recording period and found that the sleeping amount was significantly increased after ramelteon administration (Fig. 2E). This sleep-promoting effect of ramelteon was observed 60 min after administration and was maintained for at least 3 h.

To investigate the pure effect of ramelteon *per se* on neural oscillatory activity during sleep, we restricted the post-injection period to 3 h. In terms of pharmacokinetics, the elimination half-life ($t_{1/2}$) and the time (t_{max}) of the peak blood concentration (C_{max}) of ramelteon itself were less than 1 h and approximately 1 h, respectively.[15,41] Furthermore, ramelteon undergoes rapid, high first-pass metabolism. A previous study demonstrated that some metabolites of ramelteon reached approximately 10-fold higher serum concentrations relative to ramelteon[41] and suggested that the metabolites had sleep-promoting effects.[15]

In terms of extracellular oscillations, although we found a significant increase in fast gamma power only in the M1 during NREM sleep in the ramelteon-treated condition compared with the vehicle-treated condition, both fast and slow gamma powers were, overall, inclined to increase during NREM and REM sleep (Fig. 4E, F); notably, we did not find such an increase in the S1 (Fig. 4G, H). The mechanism for the M1-confined enhancement of gamma oscillations has not been empirically determined; however, we assume that one of the key brain regions for this phenomenon is the substantia nigra *pars compacta*, where dopaminergic neurons are abundant. At the cellular level, based on immunohistochemistry, MT_1 receptors are abundant exclusively in the dendrites of neurons in the substantia nigra *pars compacta*,[42] consistent with similar research at the regional level.[43] In the dopaminergic system, which includes the substantia nigra *pars compacta*, melatonin mediates the inhibition of dopamine release, possibly via MT_1 receptors.[44] A previous study using parkinsonian rats, in which medial forebrain bundles were chemically lesioned, showed that the loss of nigral dopaminergic innervation modulated the immunoreactivity of parvalbumin in the M1[45]; note that parvalbumin-immunoreactive neurons in the M1 and S1 are different in number, cell size and morphology.[46] Furthermore, it is plausible that the fast-spiking activity of parvalbumin-positive neurons generates extracellular gamma oscillations via synchronous inhibitory postsynaptic currents in cortical pyramidal cells.[47] Thus, the region-specific modulation of gamma oscillations in the ramelteon-treated group may be accounted for by the melatonin-receptor-mediated inactivation of the dopaminergic system and the subsequent activation of GABAergic neural activity.

While we assume that the MT_1 receptors were primarily involved in the enhancement of gamma oscillations in M1, another putative physiological factor that influenced neural oscillations might be the difference in the release of acetylcholine in the S1 and M1. The release of acetylcholine is higher in the S1 than the M1 in the nocturnal phase.[48] Moreover, cholinergic neurons are involved in cortical activation with desynchronized activity in electroencephalograms.[49] Thus, more desynchronization of neural activity in the S1 (compared to the M1) may underlie more variable ΔPower in the gamma oscillations in the S1 of the vehicle-treated rats.

It is also noteworthy that we did not find any modulation in power in either the delta or theta frequency bands (Fig. S1) because sedative hypnotics such as benzodiazepines and non-benzodiazepines, which act through the $GABA_A$-benzodiazepine receptor complex, increase delta power[50,51] and decrease theta power[50] possibly by positively modulating the allosteric sites of the receptor complex. Altogether, our results demonstrated that ramelteon exhibits sleep-promoting effects in a manner distinct from benzodiazepine hypnotics.

A previous study on humans demonstrated that intermittently generated gamma oscillation events were modulated by the specific phase of slow waves.[52] This phase-specific modulation of gamma events was locally coherent throughout the frontal lobe (including the primary motor area) but was not seen in the parietal lobe (including the primary somatosensory area). We speculate that this type of gamma modulation might have occurred in the local cortical network and was enhanced by ramelteon during NREM sleep in rats. Therefore, ramelteon may contribute to off-line information processing in the frontal cortical network.

Declaration of competing interest

The authors have no conflicts of interest to disclose with respect to this research.

Acknowledgments

This work was supported by JST ERATO (JPMJER1801), Institute for AI and Beyond of the University of Tokyo, and JSPS Grants-in-Aid for Scientific Research (18H05525, 20K15926).

Appendix A. Supplementary data

Supplementary data to this article can be found online at https://doi.org/10.1016/j.jphs.2020.11.006.

References

1. Griffiths RR, Sannerud CA, Ator NA, Brady JV. Zolpidem behavioral pharmacology in baboons: self-injection, discrimination, tolerance and withdrawal. *J Pharmacol Exp Therapeut*. 1992;260(3):1199–1208. http://www.ncbi.nlm.nih.gov/pubmed/1312162.
2. O'brien CP. Benzodiazepine use, abuse, and dependence. *J Clin Psychiatry*. 2005;66(Suppl 2):28–33. http://www.ncbi.nlm.nih.gov/pubmed/15762817.
3. Stewart S, Westra H. Benzodiazepine side-effects: from the bench to the clinic. *Curr Pharmaceut Des*. 2002;8(1):1–3. https://doi.org/10.2174/1381612023396708.
4. Schifano F, Chiappini S, Corkery JM, Guirguis A. An insight into Z-drug abuse and dependence: an examination of reports to the European medicines agency database of suspected adverse drug reactions. *Int J Neuropsychopharmacol*. 2019;22(4):270–277. https://doi.org/10.1093/ijnp/pyz007.
5. Terzano MG, Rossi M, Palomba V, Smerieri A, Parrino L. New drugs for insomnia: comparative tolerability of zopiclone, zolpidem and zaleplon. *Drug Saf*. 2003;26(4):261–282. https://doi.org/10.2165/00002018-200326040-00004.
6. Amaral do FG, Cipolla-Neto J. A brief review about melatonin, a pineal hormone. *Arch Endocrinol Metab*. 2018;62(4):472–479. https://doi.org/10.20945/2359-3997000000066.
7. Pévet P. Melatonin receptors as therapeutic targets in the suprachiasmatic nucleus. *Expert Opin Ther Targets*. 2016;20(10):1209–1218. https://doi.org/10.1080/14728222.2016.1179284.
8. Liu J, Clough SJ, Hutchinson AJ, Adamah-Biassi EB, Popovska-Gorevski M, Dubocovich ML. MT1 and MT2 melatonin receptors: a therapeutic perspective. *Annu Rev Pharmacol Toxicol*. 2016;56(1):361–383. https://doi.org/10.1146/annurev-pharmtox-010814-124742.
9. Hastings MH, Maywood ES, Brancaccio M. Generation of circadian rhythms in the suprachiasmatic nucleus. *Nat Rev Neurosci*. 2018;19(8):453–469. https://doi.org/10.1038/s41583-018-0026-z.
10. Miyamoto M. Pharmacology of ramelteon, a selective MT1/MT2 receptor agonist: a novel therapeutic drug for sleep disorders. *CNS Neurosci Ther*. 2009;15(1):32–51. https://doi.org/10.1111/j.1755-5949.2008.00066.x.
11. Hirai K, Kita M, Ohta H, et al. Ramelteon (TAK-375) accelerates reentrainment of circadian rhythm after a phase Advance of the light-dark cycle in rats. *J Biol Rhythm*. 2005;20(1):27–37. https://doi.org/10.1177/0748730404269890.
12. Miyamoto M, Nishikawa H, Doken Y, Hirai K, Uchikawa O, Ohkawa S. The sleep-promoting action of ramelteon (TAK-375) in freely moving cats. *Sleep*. 2004;27(7):1319–1325. https://doi.org/10.1093/sleep/27.7.1319.
13. Yukuhiro N, Kimura H, Nishikawa H, Ohkawa S, Yoshikubo S, Miyamoto M. Effects of ramelteon (TAK-375) on nocturnal sleep in freely moving monkeys. *Brain Res*. 2004;1027(1–2):59–66. https://doi.org/10.1016/j.brainres.2004.08.035.
14. Zammit G, Erman M, Wang-Weigand S, Sainati S, Zhang J, Roth T. Evaluation of the efficacy and safety of ramelteon in subjects with chronic insomnia. *J Clin Sleep Med*. 2007;3(5):495–504. https://doi.org/10.5664/jcsm.26914.
15. Fisher SP, Davidson K, Kulla A, Sugden D. Acute sleep-promoting action of the melatonin agonist, ramelteon, in the rat. *J Pineal Res*. 2008;45(2):125–132. https://doi.org/10.1111/j.1600-079X.2008.00565.x.
16. Montgomery SM, Sirota A, Buzsáki G. Theta and gamma coordination of Hippocampal networks during waking and rapid eye movement sleep. *J Neurosci*. 2008;28(26):6731–6741. https://doi.org/10.1523/JNEUROSCI.1227-08.2008.
17. Kim B, Kocsis B, Hwang E, et al. Differential modulation of global and local neural oscillations in REM sleep by homeostatic sleep regulation. *Proc Natl Acad Sci*. 2017;114(9):E1727–E1736. https://doi.org/10.1073/pnas.1615230114.
18. Le Van Quyen M, Muller LE, Telenczuk B, et al. High-frequency oscillations in human and monkey neocortex during the wake–sleep cycle. *Proc Natl Acad Sci*. 2016;113(33):9363–9368. https://doi.org/10.1073/pnas.1523583113.
19. Le Van Quyen M, Staba R, Bragin A, et al. Large-scale microelectrode recordings of high-frequency gamma oscillations in human cortex during sleep. *J Neurosci*. 2010;30(23):7770–7782. https://doi.org/10.1523/JNEUROSCI.5049-09.2010.
20. Moran LV, Hong LE. High vs low frequency neural oscillations in schizophrenia. *Schizophr Bull*. 2011;37(4):659–663. https://doi.org/10.1093/schbul/sbr056.
21. Okada S, Igata H, Sakaguchi T, Sasaki T, Ikegaya Y. A new device for the simultaneous recording of cerebral, cardiac, and muscular electrical activity in freely moving rodents. *J Pharmacol Sci*. 2016;132(1):105–108. https://doi.org/10.1016/j.jphs.2016.06.001.
22. Sasaki T, Nishimura Y, Ikegaya Y. Simultaneous recordings of central and peripheral bioelectrical signals in a freely moving rodent. *Biol Pharm Bull*. 2017;40(5):711–715. https://doi.org/10.1248/bpb.b17-00070.
23. Shikano Y, Sasaki T, Ikegaya Y. Simultaneous recordings of cortical local field potentials, electrocardiogram, electromyogram, and breathing rhythm from a freely moving rat. *J Vis Exp*. 2018;134. https://doi.org/10.3791/56980.
24. Kuga N, Nakayama R, Shikano Y, et al. Sniffing behaviour-related changes in cardiac and cortical activity in rats. *J Physiol*. 2019;597(21):5295–5306. https://doi.org/10.1113/JP278500.
25. Geiger BM, Frank LE, Caldera-Siu AD, Pothos EN. Survivable stereotaxic surgery in rodents. *J Vis Exp*. 2008;20. https://doi.org/10.3791/880.
26. Drummond LR, Kunstetter AC, Vaz FF, et al. Brain temperature in spontaneously hypertensive rats during physical exercise in temperate and warm environments. González GE. *PLoS One*. 2016;11(5), e0155919. https://doi.org/10.1371/journal.pone.0155919.
27. Ferraro L, Tomasini MC, Cassano T, et al. Cannabinoid receptor agonist WIN 55,212-2 inhibits rat cortical dialysate?-aminobutyric acid levels. *J Neurosci Res*. 2001;66(2):298–302. https://doi.org/10.1002/jnr.1224.
28. Vyazovskiy VV, Faraguna U, Cirelli C, Tononi G. Triggering slow waves during NREM sleep in the rat by intracortical electrical stimulation: effects of sleep/wake history and background activity. *J Neurophysiol*. 2009;101(4):1921–1931. https://doi.org/10.1152/jn.91157.2008.
29. Vyazovskiy VV, Olcese U, Hanlon EC, Nir Y, Cirelli C, Tononi G. Local sleep in awake rats. *Nature*. 2011;472(7344):443–447. https://doi.org/10.1038/nature10009.
30. Yamashiro K, Aoki M, Matsumoto N, Ikegaya Y. Polyherbal formulation enhancing cerebral slow waves in sleeping rats. *Biol Pharm Bull*. 2020;43(9):1356–1360. https://doi.org/10.1248/bpb.b20-00285.
31. Siegle JH, López AC, Patel YA, Abramov K, Ohayon S, Voigts J. Open Ephys: an open-source, plugin-based platform for multichannel electrophysiology. *J Neural Eng*. 2017;14(4), 045003. https://doi.org/10.1088/1741-2552/aa5eea.
32. Sato M, Matsumoto N, Noguchi A, Okonogi T, Sasaki T, Ikegaya Y. Simultaneous monitoring of mouse respiratory and cardiac rates through a single precordial electrode. *J Pharmacol Sci*. 2018;137(2):177–186. https://doi.org/10.1016/j.jphs.2018.06.009.
33. Bagur S, Lacroix MM, de Lavilléon G, Lefort JM, Geoffroy H, Benchenane K. Harnessing olfactory bulb oscillations to perform fully brain-based sleep-scoring and real-time monitoring of anaesthesia depth. Timofeev I. *PLoS Biol*. 2018;16(11), e2005458. https://doi.org/10.1371/journal.pbio.2005458.
34. Mizuseki K, Diba K, Pastalkova E, Buzsáki G. Hippocampal CA1 pyramidal cells form functionally distinct sublayers. *Nat Neurosci*. 2011;14(9):1174. https://doi.org/10.1038/nn.2894.
35. Tartar JL, Ward CP, McKenna JT, et al. Hippocampal synaptic plasticity and spatial learning are impaired in a rat model of sleep fragmentation. *Eur J Neurosci*. 2006;23(10):2739–2748. https://doi.org/10.1111/j.1460-9568.2006.04808.x.
36. Rangel LM, Chiba AA, Quinn LK. Theta and beta oscillatory dynamics in the dentate gyrus reveal a shift in network processing state during cue encounters. *Front Syst Neurosci*. 2015;9. https://doi.org/10.3389/fnsys.2015.00096.
37. Samson RD, Lester AW, Duarte L, Venkatesh A, Barnes CA. Emergence of β-band oscillations in the aged rat amygdala during discrimination learning and decision making tasks. *eneuro*. 2017;4(5). https://doi.org/10.1523/ENEURO.0245-17.2017. ENEURO.0245-17.2017.
38. Bertrand SJ, Zhang Z, Patel R, et al. Transient neonatal sleep fragmentation results in long-term neuroinflammation and cognitive impairment in a rabbit model. *Exp Neurol*. 2020;327:113212. https://doi.org/10.1016/j.expneurol.2020.113212.
39. Gobbi G, Comai S. Differential function of melatonin MT_1 and MT_2 receptors in REM and NREM sleep. *Front Endocrinol (Lausanne)*. 2019;10. https://doi.org/10.3389/fendo.2019.00087.
40. Vyazovskiy VV, Cui N, Rodriguez AV, Funk C, Cirelli C, Tononi G. The dynamics of cortical neuronal activity in the first minutes after spontaneous awakening in rats and mice. *Sleep*. 2014;37(8):1337–1347. https://doi.org/10.5665/sleep.3926.
41. Karim A, Tolbert D, Cao C. Disposition kinetics and tolerance of escalating single doses of ramelteon, a high-affinity MT_1 and MT_2 melatonin receptor agonist indicated for treatment of insomnia. *J Clin Pharmacol*. 2006;46(2):140–148. https://doi.org/10.1177/0091270005283461.
42. Lacoste B, Angeloni D, Dominguez-Lopez S, et al. Anatomical and cellular localization of melatonin MT_1 and MT_2 receptors in the adult rat brain. *J Pineal Res*. 2015;58(4):397–417. https://doi.org/10.1111/jpi.12224.
43. Uz T, Arslan AD, Kurtuncu M, et al. The regional and cellular expression profile of the melatonin receptor MT1 in the central dopaminergic system. *Mol Brain Res*. 2005;136(1–2):45–53. https://doi.org/10.1016/j.molbrainres.2005.01.002.
44. Zisapel N. Melatonin-dopamine interactions: from basic neurochemistry to a clinical setting. *Cell Mol Neurobiol*. 2001;21:605–616. https://doi.org/10.1023/A:1015187601628.
45. Capper-Loup C, Burgunder J-M, Kaelin-Lang A. Modulation of parvalbumin expression in the motor cortex of parkinsonian rats. *Exp Neurol*. 2005;193(1):234–237. https://doi.org/10.1016/j.expneurol.2004.12.007.
46. van Brederode JFM, Helliesen MK, Hendrickson AE. Distribution of the calcium-binding proteins parvalbumin and calbindin-D28k in the sensorimotor cortex of the rat. *Neuroscience*. 1991;44(1):157–171. https://doi.org/10.1016/0306-4522(91)90258-P.
47. Buzsáki G, Wang X-J. Mechanisms of gamma oscillations. *Annu Rev Neurosci*. 2012;35(1):203–225. https://doi.org/10.1146/annurev-neuro-062111-150444.
48. Jiménez-Capdeville ME, Dykes RW. Changes in cortical acetylcholine release in the rat during day and night: differences between motor and sensory areas. *Neuroscience*. 1996;71(2):567–579. https://doi.org/10.1016/0306-4522(95)00439-4.
49. Blake MG, Boccia MM. Basal forebrain cholinergic system and memory. In: Clark RE, Martin S, eds. *Current topics in behavioral neurosciences*. Cham: Springer; 2016:253–273. https://doi.org/10.1007/7854_2016_467.
50. Renger JJ, Dunn SL, Motzel SL, Johnson C, Koblan KS. Sub-chronic administration of zolpidem affects modifications to rat sleep architecture. *Brain Res*. 2004;1010(1–2):45–54. https://doi.org/10.1016/j.brainres.2004.02.067.
51. Noguchi H, Kitazumi K, Mori M, Shiba T. Electroencephalographic properties of zaleplon, a non-benzodiazepine sedative/hypnotic, in rats. *J Pharmacol Sci*. 2004;94(3):246–251. https://doi.org/10.1254/jphs.94.246.
52. Valderrama M, Crépon B, Botella-Soler V, et al. Human gamma oscillations during slow wave sleep. Sporns O. *PLoS One*. 2012;7(4), e33477. https://doi.org/10.1371/journal.pone.0033477.